

Hybrid FEM-BEM for simulation of electromagnetic response

Yu Haitao

(Department of Electrical Engineering, Southeast University, Nanjing 210096, China)

Abstract: A finite element method with boundary element method (FEM-BEM) is presented for computing electromagnetic induction. The features of an edge element method including the volume and surface edge element method are investigated in depth. Surface basis functions of edge elements to an arbitrary shape of target are derived according to the geometrical property of basis functions and applied to discretize the surface integral equation for 3-D general targets. The proposed model is presented to compute resonant frequencies and surface current of underground unexplored ordnance (UXO), and then the electromagnetic responses of single target with different frequencies and positions of sensor are simulated and results are validated by experiments.

Key words: hybrid FEM-BEM; underground unexplored ordnance; electromagnetic response

The detection of unexplored ordnance (UXO)^[1,2], such as buried landmines and missiles, is the work of well-known humanitarian importance. Electromagnetic induction (EMI) is widely used to sensor and discriminate UXO targets, especially for those made of metal and ferrite^[2]. As we know, an object has its own series of resonant frequencies^[3], but the electromagnetic response at the first resonant frequency is very strong so that searching it becomes very important to identify the features of objects. In high frequency electromagnetics, the dielectric or loss targets are usually investigated for designing microwave components or waveguide, whose resonant frequency is very high, an order of 300 MHz or so. However, if the conductivity of targets becomes high, for example well-conducting metal, the real part of the resonant frequency is close to zero and the imaginary becomes large. High frequency formulations at this time cannot get convergent solutions^[2] when we implemented method of moment (MoM) code for the solution of the resonance.

FEM-BEM^[4,5] is one of the most powerful solvers used in low frequency electromagnetics. FEM^[6-8] can be used to deal with complex target shapes and inhomogeneous media while BEM is used to cut down the computational area; therefore minimal unknowns are used in the electromagnetic computation. Edge element method has been implemented to FEM formulation since this numerical method was proposed in 1980s. This method allows vector fields directly to be variables as only tangential component on the adjacent elements is constrained to

be continuous. However, edge element method is seldom applied to BEM although some authors^[9,10] successfully calculated eddy currents for specific target shape, such as rectangle. Therefore, the establishment of the surface basis function of edge elements, only involved in one local triangle patch, for the surface integral equation is significant to the **electromagnetic computation of general targets**.

1 Edge Element Method

As we know, the nodal based element is the fundamental element among four elements: nodes, elements, facets and volume^[10-12]. Any other element is expressed by using the basis functions of the nodal based element. Here we are interested in the edge element methods including the volume method and the **surface edge element method**.

1.1 Three-dimensional edge element method

The numerical computation we perform in the whole area becomes the computation at each local sub-region, and the final results are obtained by the summation of the result at each local element according to the characteristics of numerical methods. In order to penetrate into the truth of 0-simplex^[11] and extend this to the application of higher P -simplex, suppose that a tetrahedron with four vertices P_i having Cartesian coordinates (x_i, y_i, z_i) , $i = 1, 2, 3, 4$, is shown in Fig. 1. Let point P have Cartesian coordinates (x, y, z) within the tetrahedron, therefore the original tetrahedron is subdivided into four smaller tetrahedrons. The local coordinates concerning P are defined by four basis functions $(\lambda_1, \lambda_2, \lambda_3, \lambda_4)$. The first order of basis functions is linear corresponding with point $P(x, y, z)$, for

Received 2004-03-31.

Biography: Yu Haitao (1965—), male, doctor, professor, htyu@seu.edu.cn.

example,

$$\lambda_1 = \frac{1}{3V} \begin{vmatrix} 1 & x & y & z \\ 1 & x_2 & y_2 & z_2 \\ 1 & x_3 & y_3 & z_3 \\ 1 & x_4 & y_4 & z_4 \end{vmatrix} = \frac{\mathbf{A}_1 \mathbf{R}_{P_4 P}}{3V} \quad (1)$$

where \mathbf{A}_1 is the area vector of $\Delta P_2 P_3 P_4$, and $\mathbf{R}_{P_4 P}$ is a vector from P_4 to P .

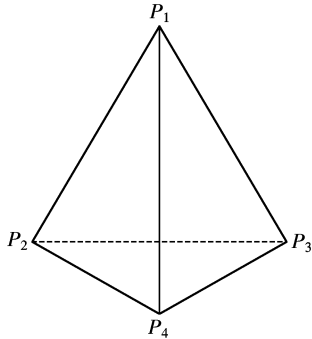


Fig.1 A tetrahedron element

We now get a basis function of vector space N^1 along edge $e = \{i, j\}$,

$$N_e = \lambda_i \nabla \lambda_j - \lambda_j \nabla \lambda_i \quad (2)$$

For example,

$$N_1 = \frac{\mathbf{A}_1 \times \mathbf{A}_2}{9V^2} \times \mathbf{R}_{PP_4} \quad (3)$$

where \mathbf{A}_2 is the area of $\Delta P_1 P_4 P_3$. Eq. (3) is a basis function of the edge element method.

1.2 Surface edge element method

In order to propose the surface edge elements, we first investigate the nodal basis functions at a triangle patch. Suppose $\Delta P_2 P_3 P_4$ lies on xoy plane. We can easily get nodal basis functions in two dimensions. We write one of the nodal basis functions as

$$\lambda_1 = \frac{1}{2A} \begin{vmatrix} 1 & x & y \\ 1 & x_3 & y_3 \\ 1 & x_4 & y_4 \end{vmatrix} \quad (4)$$

where A is the area of a triangle.

After we compare Eq. (4) with linear equation of the corresponding edge, we know that the nodal basis function is a normalized corresponding linear equation, for example, λ_1 is the linear equation of edge $\{P_2, P_3\}$.

We now consider the case that $\Delta P_2 P_3 P_4$ is on the surfaces of a general object without any of its sides parallel to x , y or z axis.

According to the definition, we write the nodal basis function of the triangle element as a linear equation to position P :

$$\lambda_{si} = a_i + b_i x + c_i y + d_i z \quad (5)$$

But at this time Eq. (5) is equivalent to the

equation of a plane through an edge of the triangle (shown in Fig.2). We choose the plane that is vertical to the triangle element as a nodal surface basis function:

$$\{b_i, c_i, d_i\} \cdot \hat{\mathbf{n}} = \{b_i, c_i, d_i\} \cdot \{n_x, n_y, n_z\}^T = 0 \quad (6)$$

where n_x, n_y, n_z are three normalized components of \mathbf{n} , and (x, y, z) in Eq. (5) is the position of P . We get three groups of coefficients through the features of basis functions:

$$\begin{bmatrix} 1 & x_1 & y_1 & z_1 \\ 1 & x_2 & y_2 & z_2 \\ 1 & x_3 & y_3 & z_3 \\ 0 & n_x & n_y & n_z \end{bmatrix} \begin{Bmatrix} a_i \\ b_i \\ c_i \\ d_i \end{Bmatrix} = \begin{Bmatrix} k_{i1} \\ k_{i2} \\ k_{i3} \\ 0 \end{Bmatrix} \quad (7)$$

where

$$k_{ij} = \begin{cases} 0 & i \neq j \\ 1 & i = j \end{cases}$$

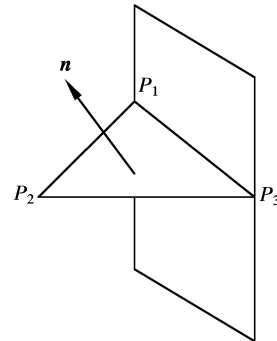


Fig.2 A triangular element

Finally, three basis functions of nodal basis function are obtained for a triangle element at any position. It is not difficult to verify that the new basis functions have the same features as other nodal based elements in two dimensions and three dimensions, for example,

$$\sum_{i=1}^3 \lambda_{si} = 1 \quad (8)$$

Substituting Eq. (5) which is got from Eq. (7) into the formulation of edge elements^[10], we get surface basis function N_{se} along edge $e = \{i, j\}$,

$$N_{se} = \lambda_{si} \nabla \lambda_{sj} - \lambda_{sj} \nabla \lambda_{si} \quad (9)$$

We derive the following identity with Eq. (9)

$$N_{se} \cdot \vec{ij} \equiv \pm 1 \quad (10)$$

which makes sure that the tangential component of vectors is continuous between two adjacent elements.

We implement edge elements to interpolate the electrical current \mathbf{J} and magnetic current \mathbf{M} on the surface integration:

$$\mathbf{J} = \sum_{e=1}^3 \mathbf{J}_e = \sum_{e=1}^3 \mathbf{n} \times \mathbf{H}_e = \sum_{e=1}^3 \mathbf{n} \times N_{se} \mathbf{H}_e \quad (11)$$

$$\mathbf{M} = \sum_{e=1}^3 \mathbf{M}_e = - \sum_{e=1}^3 \mathbf{n} \times \mathbf{E}_e =$$

$$j\omega\mu_0 \sum_{e=1}^3 \mathbf{n} \times \mathbf{N}_{se} A_e \quad (12)$$

where H_e is an edge variable corresponding to the magnetic density, and A_e is the equivalent magnetic potential which we will explain in the next section. Like volume edge elements, basis function N_{se} keeps the tangential component continuous along an edge, while $\mathbf{n} \times \mathbf{N}_{se}$ is also a constant at the normal direction to edge $e = \{i, j\}$ and keeps currents continuous on the adjacent elements. The electric and magnetic currents continuous in the normal direction meet the properties of electromagnetics so that this method can be applied to the EM formulations.

2 Formulations

Fig.3 shows the electromagnetic problem investigated in this paper. Ω_1 is a 3-D general target enclosed by surface Γ , in which the parameters are conductivity σ , permeability μ , and permittivity ε . Ω_2 is non-conducting region, where the parameters are permeability μ_0 , permittivity ε_0 , and current density \mathbf{J}_0 is supplied in free space.

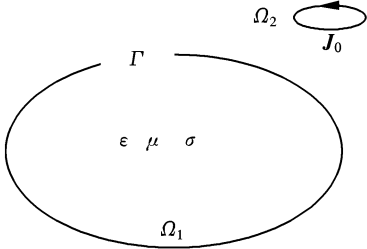


Fig.3 EM problem configuration

2.1 Inside an object

We implement FEM in region Ω_1 and set the magnetic field and vector magnetic potential as physical variables. The governing equation is given as follows:

$$\nabla \times \frac{1}{\sigma + j\omega\varepsilon} \nabla \times \mathbf{H} = -j\omega\mu\mathbf{H} \quad (13)$$

With vector identities, Eq.(13) is rewritten as

$$\mathbf{W}_e \cdot \nabla \times \nabla \times \mathbf{H} = \nabla \times \mathbf{W}_e \cdot \nabla \times \mathbf{H} + j\omega\mu_0(\sigma + j\omega\varepsilon) \nabla \cdot (\mathbf{W}_e \times \mathbf{A}) \quad (14)$$

where $\mathbf{A} = \mathbf{A}^*/\mu_0$, \mathbf{A}^* is the reduced magnetic potential. \mathbf{A} is introduced in order to make coefficients of terms in the integral equation presented in the next section very close to each other.

Applying the Galerkin method to Eq. (14), we have

$$\int_{\Omega} \nabla \times \mathbf{W}_e \cdot \nabla \times \mathbf{H} dV + j\omega\mu(\sigma + j\omega\varepsilon) \times$$

$$\int_{\Omega} \mathbf{W}_e \cdot \mathbf{H} dV + j\omega\mu_0(\sigma + j\omega\varepsilon) \times \oint_{\Gamma} (\hat{\mathbf{n}} \times \mathbf{A}) \cdot \mathbf{W}_e dS = 0 \quad (15)$$

where \mathbf{W}_e is the weighting function equal to the vector basis function of edge elements, and $\hat{\mathbf{n}}$ is the outward normal unit vector to interface.

By implementing edge elements within a tetrahedron^[5,10], vector \mathbf{H} is interpolated as

$$\mathbf{H} = \sum_{e=1}^6 \mathbf{N}_e H_e \quad (16)$$

where H_e is a variable on edge $e = \{i, j\}$, defined as the integral of vector \mathbf{H} on edge e .

The third term in Eq.(15) exists on the interface, therefore surface basis function is used to interpolate \mathbf{A} ,

$$\hat{\mathbf{n}} \times \mathbf{A} = \hat{\mathbf{n}} \times \sum_{e=1}^3 \mathbf{N}_{se} A_e \quad (17)$$

where A_e is a variable, the integral of magnetic potential on edge $e = \{i, j\}$, and \mathbf{N}_{se} is the surface basis function along edge $e = \{i, j\}$. Two variables H and A are used to an edge on the surface integration, but one variable is only required on each edge inside the target.

Linear equations in the conducting region are obtained after discretion of Eq.(15) by edge elements,

$$\{M_{ee'} + T_{ee'}, S_{ee'}\} \begin{Bmatrix} H \\ A \end{Bmatrix} = 0 \quad (18)$$

where the coefficient matrix is sparse and asymmetric.

2.2 On the surface of an object

On the surface of the target, surface edge element method in Eq. (9) is used to interpolate the integral formulation. H and A are set as physical quantities. The governing integral equation for this region is derived from Green's theorem as follows^[9]:

$$C_p \mathbf{H}_e = \int_{\Omega} \mathbf{J}_0 \times \nabla G dS' - j\omega\varepsilon_0 \oint_{\Gamma} (\hat{\mathbf{n}} \times \mathbf{E}) G dS' - \oint_{\Gamma} (\hat{\mathbf{n}} \times \mathbf{H}) \times \nabla G dS' - \oint_{\Gamma} (\hat{\mathbf{n}} \cdot \mathbf{H}) \nabla G dS' \quad (19)$$

Substituting $\mathbf{H} = \nabla \times \mathbf{A}$ and $\mathbf{E} = -j\omega\mu_0 \mathbf{A}$ into Eq.(19), we get

$$C_p \mathbf{H}_e = \int_{\Omega} \mathbf{J}_0 \times \nabla G dS' + k_0^2 \oint_{\Gamma} (\hat{\mathbf{n}} \times \mathbf{A}) G dS' - \oint_{\Gamma} (\hat{\mathbf{n}} \times \mathbf{H}) \times \nabla G dS' - \oint_{\Gamma} (\hat{\mathbf{n}} \cdot \nabla \times \mathbf{A}) \nabla G dS' \quad (20)$$

where C_p is the solid angle subtended by the analyzed region at a source point; $C_p = 0$ if the observation point is inside a target; $C_p = 0.5$ if the observation point is on target surface; $C_p = 1$ if the observation point is outside the target. Since C_p is introduced, the singularity problem is removed automatically. However, analytical expressions are still required for accurate solutions when the observation point and source point are close to each other, for example, if the distance is less than half of the wavelength.

G in Eqs.(19) and (20) is Green's function,

$$G = \frac{\exp(-jk_0 |\mathbf{r}_i - \mathbf{r}_{i'}|)}{4\pi |\mathbf{r}_i - \mathbf{r}_{i'}|} \quad (21)$$

where \mathbf{r}_i and $\mathbf{r}_{i'}$ are the positions of observation and source point, respectively, and k_0 is the propagation constant^[1].

The first term on the right hand of Eq. (20) expresses the incident magnetic field induced by sensors. The second term stands for the magnetic field produced by the surface magnetic current but the effect of this term is much less in low frequency than that in high frequency. The coefficients at the third and the fourth terms are not functions of frequency, and therefore Eq. (20) is variable to wide-band electromagnetics.

Applying the Galekin method and setting weighting function $\mathbf{W}_{se} = \mathbf{N}_{se} \times \hat{\mathbf{n}}$, we get coefficient matrices of Eq.(20). Combining to Eq.(15), we get the linear equations in the whole problem region,

$$\mathbf{Z} \begin{Bmatrix} H \\ A \end{Bmatrix} = \begin{Bmatrix} 0 \\ B_e \end{Bmatrix} \quad (22)$$

where \mathbf{Z} is the FEM-BEM coefficient matrix. Since the impedance matrix of BEM is full scale, the final impedance \mathbf{Z} is no longer sparse. Natural resonant frequency is characterized by a zero determinant of impedance matrix:

$$|\mathbf{Z}| = 0 \quad (23)$$

Eq.(23) means that resonance is independent of driven source. Resonant frequency is nothing with excitation but dependent on target shapes, sizes and material features. The solution can be got by solving eigenvalues, but we are only interested in the first resonant frequency so the direct method to solve this problem is to search for a zero determinant along the imaginary part of the frequency axis. However, the computational errors make the determinant nonzero but very close to zero. In order to confirm that the frequency is the one we are looking for, we calculate the distribution of surface electric currents at this

frequency as different resonances having different surface current distributions.

3 Examples

3.1 Free source response of a cuboid

The first example of FEM-BEM application is to compute resonant frequencies of a cuboid with sides measuring, 1.27, 1.27, and 7.62 cm long, respectively. The conductivity of the cuboid is 5.6 MS/m. The frequency characterization of the cuboid is shown in Fig. 4. The first resonant frequency is around 1 367 Hz and the second one is 1 415 Hz. The surface electric current plotted in Fig.5 has only one peak to confirm that frequency 1 367 Hz is the lowest resonant frequency.

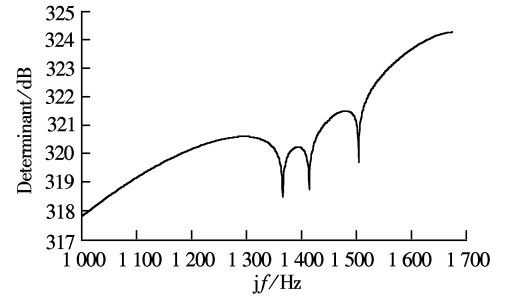


Fig.4 Imaginary frequency features of a cuboid

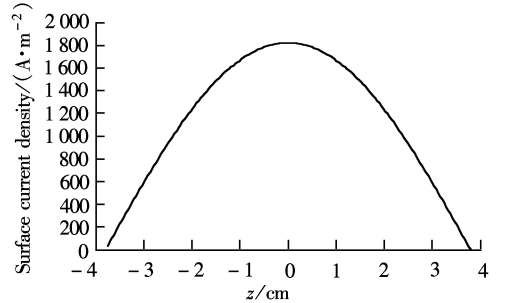


Fig.5 Electric current density along z axis at the lowest resonant frequency

3.2 EMI response from a cube

We now perform numerical computations to investigate EMI response, which is another method to detect unexplored underground targets. The computational mode is shown in Fig.6. The cube, 0.1 m on each side is made of stainless steel, with conductivity of 1.3 MS/m. The distance between the cube and the center of the sensor is 0.5 m. The sensor plotted in Fig. 6 is GEM-3 including source and receiving loops. We tested EMI responses with frequency arrange from 10 Hz to 10 kHz and with different angles ϕ from 0° to 180° , respectively.

We carried out experiments and computed the EMI response with the proposed method, and both results shown in Fig. 7 agree with each other very

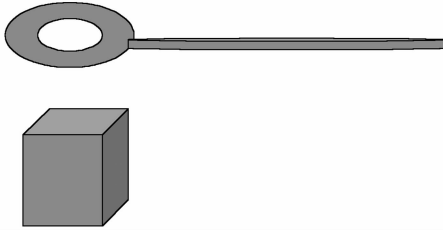


Fig.6 EMI response from a cube

well. The frequency-domain EMI response of a conducting or ferrous target is characterized by resonant frequencies at which the imaginary part of EMI response is the maximum. The real part of EMI response becomes large when the frequency increases but its increment will be less and less and finally close to zero if the frequency is big enough. The frequency features of EMI response separated as the real part and the imaginary part can be seen in Fig. 7. The frequency at the cross-point between the real part and the imaginary part is considered as the lowest resonant frequency.

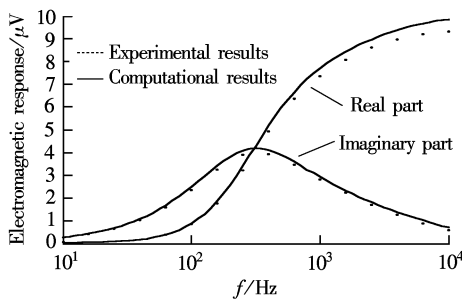


Fig.7 Frequency feature of EMI response

The results shown in Fig. 8 were obtained with the motion of the sensor along y axis from -0.5 to 0.5 m. The peak of the waveform appears when the sensor is close to the target. From Figs. 7 and 8, we can see that the computational results match the experimental ones very well so that the proposed numerical method is valid for the computation of EMI response.

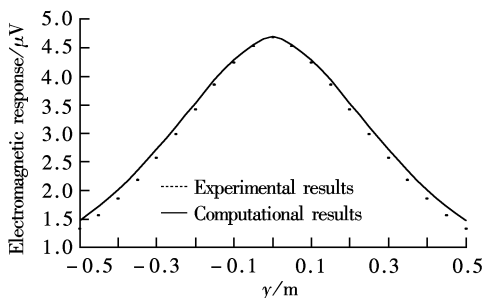


Fig.8 EMI response along y axis

4 Conclusion

A surface edge element method has been successfully proposed and implemented to BEM

formulation. A hybrid mathematical model has been presented for 3-D wide-band electromagnetic induction response from general conducting targets. Finally, the proposed method has been used to compute the resonant frequency and electromagnetic response and the results matched those from the experiment so that it is an efficient method in the electromagnetic computation.

References

- [1] Balanis Constantine A. *Advanced engineering electromagnetics* [M]. New York: Wiley, 1989.
- [2] Carin L, Yu H T. On the wide-band EMI response of a rotationally symmetric permeable and conducting target [J]. *IEEE Transactions on Geoscience & Remote Sensing*, **2001**, **39**(6): 1206 – 1213.
- [3] Glisson A W, Kajfez D, James J. Evaluation of modes in dielectric resonators using a surface integral equation formulation [J]. *IEEE Transactions on Microwave Theory and Techniques*, **1983**, **31**(12): 1023 – 1029.
- [4] Lu Yilong, Fernandez F Anibal. An efficient finite element solution of inhomogeneous anisotropic and lossy dielectric waveguides [J]. *IEEE Transactions on Microwave Theory and Techniques*, **1993**, **41** (6): 1215 – 1223.
- [5] Yuan X, Lynch D R, Strohbehm J W. Coupling of finite element and moment methods for electromagnetic scattering from inhomogeneous objects [J]. *IEEE Trans Antennas Propagat*, **1990**, **38**(3): 386 – 393.
- [6] Andersen L S, Volakis J L. Development of application of novel class of hierarchical tangential vector finite elements for electromagnetics [J]. *IEEE Trans Antennas Propagat*, **1999**, **47**(3): 112 – 120.
- [7] Pichon Lionel. Comparison between tangentially continuous vector finite elements for eigenvalue problems in 3-D cavities [J]. *IEEE Transactions on Magnetics*, **1996**, **33**(3): 902 – 905.
- [8] Wolfe C T, Navsariwala U, Gedney Stephen D. A parallel finite-element tearing and interconnecting algorithm for solution of the vector wave equation with PML absorbing medium [J]. *IEEE Trans Antennas Propagat*, **2000**, **48**(2): 278 – 283.
- [9] Wakao S, Onuki T. Electromagnetic field computations by the hybrid FE-BE method using edge elements [J]. *IEEE Transactions on Magnetics*, **1992**, **29**(2): 1487 – 1490.
- [10] Rucker W M, Richter K R. A BEM code for 3-D eddy current calculations [J]. *IEEE Transactions on Magnetics*, **1989**, **26**(2): 462 – 465.
- [11] Nedelec J C. Mixed finite element in R^3 [J]. *Numer Math*, **1980**, **35**(2): 315 – 341.
- [12] Bossavit A, Mayergoyz I D. Edge elements for scattering problems [J]. *IEEE Transactions on Magnetics*, **1989**, **25** (4): 2816 – 2821.

有限元-边界元法计算电磁响应

余海涛

(东南大学电气工程系, 南京 210096)

摘要: 提出了用有限元-边界元法计算三维电磁场感应问题. 首先阐述了棱边单元法的基本性质, 并且根据基函数的几何平面特性推导出对于任意位置面的表面棱边单元法基本公式, 然后用棱边单元法离散数学模型. 用此方法模拟地下金属军事目标的电磁响应, 计算了目标的最低谐振频率及表面电流密度, 和单一目标的频率特性及位移特性, 计算结果和实验结果一致, 因此这种数值方法对计算三维电磁场问题行之有效.

关键词: 有限元-边界元混合方法; 地下军事目标; 电磁响应

中图分类号: TM154